International Journal for Housing Science and Its Applications
Publish August 10, 2025. Volume 46, Issue 4 Pages 1872-1887

https://doi.org/10.70517/ijhsa464162

A Model for Evaluating the Effectiveness of Ideological and Political Education Assisted by Biosensing Technology

Yue You[1], Mingyue Zhang[2,*] and Luchang Yang[3]
[1] School of Fine Arts and Design, Hebei Minzu Normal University, Chengde, Hebei, 067000, China
[2] Tianjin-Chengde Art Design Department, Chengde College of Applied Technology, Chengde, Hebei, 067000, China
[3] School of Mathematics and Computer Science, Hebei Minzu Normal University, Chengde, Hebei, 067000, China
Corresponding authors: (e-mail: zhangmingyue824@163.com).

Abstract With the rapid development of biosensing technology, the field of ideological and political education has also ushered in a new era of intelligent education. This paper proposes a method for evaluating the effectiveness of ideological and political education by combining facial expression and behavior recognition of college students. First, a student facial expression recognition model based on a deep attention network is proposed. This model learns the facial expression features of students, fuses multiple facial expression features, and classifies them. A student behavior recognition algorithm based on multi-task learning is proposed, using an object detector to extract data from videos as algorithm input. Through a multi-task heatmap network module, intermediate heatmaps are extracted and encoded into private heatmaps to obtain student joint position information. Subsequently, behavior vectors and metric vectors are introduced to model student classroom behavior separately. The obtained behavior states are combined with expression categories, and the two types of data are jointly input into the model for training, enabling dynamic evaluation of the effectiveness of ideological and political education for students. Experiments show that the evaluation model integrating expressions and behaviors achieves an accuracy rate of 85.44%, effectively overcoming evaluation biases caused by single-dimensional features. In practical applications, the model achieves an overall evaluation accuracy rate of 94%, comparable to manual detection levels, providing efficient and intelligent technical support for ideological and political classroom teaching.

Index Terms deep attention network, expression recognition, behavior recognition, multi-task heatmap network, ideological and political education effectiveness evaluation

I. Introduction

University ideological and political education is a crucial component of the higher education system, aimed at cultivating college students' ideological and moral qualities, innovative thinking, and sense of social responsibility, enabling them to adapt to the demands of societal development and contribute to societal progress [1]-[4]. The significance of evaluating the effectiveness of ideological and political education lies in identifying issues, addressing challenges, enhancing teaching quality, and improving educational standards to provide students with superior ideological and political education [5], [6].

Currently, evaluations of the effectiveness of ideological and political education often rely on traditional methods such as questionnaire surveys and statistical analysis of student grades. These methods have certain limitations when it comes to assessing students' ideological and political literacy and moral emotions [7]-[9]. In response to this issue, an evaluation method based on biosensing technology has emerged [10], [11]. Biological sensing technology is a high-tech field that has emerged through the integration of multiple disciplines such as biology, chemistry, physics, medicine, and electronics. It holds significant application value in fields such as biomedicine, environmental monitoring, food, pharmaceuticals, and military medicine [12]-[15]. The 21st century is the era of life sciences. With the completion of the “Human Genome Project,” the emergence of nanobiotechnology, and nanoscale electronic processing technology, both in terms of principles and processing techniques, these advancements will bring significant transformations to biosensing technology [16]-[19]. In the evaluation of the effectiveness of ideological and political education in universities, by constructing an evaluation model and analyzing students' professional abilities and ideological and political literacy, it is possible to more accurately grasp students' learning status and the improvement of their ideological and political literacy, providing teachers with more scientific teaching guidance and evaluation criteria for students, and offering strong support for educational and teaching work [20]-[23].

Literature [24] elaborates on the significance of ideological and political education effectiveness evaluation, conducts data collection and analysis based on questionnaire surveys, and uses independent t-tests, multiple regression, and chiseling methods to verify hypotheses. Finally, it discusses the content of students' ideological and political education learning, commonly used evaluation methods, and students' ideological and political literacy levels. Literature [25] uses the analytic hierarchy process to construct multiple evaluation indicators and a recursive hierarchical structure model for evaluating the effectiveness of ideological and political education on university WeChat official accounts. It uses a two-level evaluation method to determine the weight values of each indicator. The research results not only facilitate improvements to university new media education platforms but also provide references for enhancing teaching quality. Literature [26] analyzed evaluation methods for university ideological and political education and proposed an innovative framework combining outcome-based education with context, input, process, and product models, offering new insights and references for evaluating university ideological and political education. Literature [27] studied speech recognition and university ideological and political education quality assessment based on mobile biosensor networks, demonstrating consistency with previous research and revealing the positive role of cellular networks in strengthening ideological and political education for college students. Literature [28] discusses the application of biosensor technology in ideological and political education assessment and emphasizes the important role of mental health education for students. Based on this, it proposes a student evaluation model generated from biosensor data, facial emotion recognition, and electroencephalogram (EEG) signals, revealing the effectiveness of biosensor technology in ideological and political education assessment. Literature [29] explores the effectiveness of biosensor technology in enhancing the dissemination of health information within ideological and political education and employs an improved Runge-Kutta optimizer and deep belief network classifier to predict student engagement, revealing the effectiveness of biosensor technology. Student physiological responses, particularly heart rate variability and skin conductance, are closely correlated with student engagement. Literature [30] aims to establish a bio-sensor-based emotional monitoring and feedback system for ideological and political education, proposing a novel “battle royale” fine-tuned deep bidirectional long short-term memory to detect students' cognitive and emotional engagement, revealing the system's potential to enhance participation in ideological and political education through adaptive feedback mechanisms based on sensor data. Literature [31] explores the application of biomechanics-based biosensing technology in psychological analysis to enhance the efficiency of ideological and political education. By utilizing multi-core support vector machines to assess students' physical strain levels during activities, the study validated the effectiveness of this method, demonstrating superior accuracy and precision compared to traditional approaches. Literature [32] aims to provide biofeedback on emotions to assess the effectiveness of ideological and political education and ideological dissemination. By proposing a new adaptive deep belief network model driven by random fractal search, it predicts and evaluates students' emotional and attentional characteristics, revealing that this method outperforms traditional methods.

To overcome the limitations of current ideological and political education effectiveness assessment, which heavily relies on one-dimensional data and struggles to objectively quantify student learning outcomes, this paper proposes a dual-modal student education effectiveness assessment framework based on biosensing technology. The facial expression feature learning module based on a deep attention convolutional neural network extracts students' facial expression features, while the attention feature weight allocation module assigns different weights. A softmax classifier is used to classify the learned facial expressions. The student behavior recognition algorithm uses ideological and political classroom teaching videos as data sources to obtain individual student data. Subsequently, a multi-task heatmap network is used to generate shared heatmaps. Then, through DCT and DNN modules, student behavior is identified. Both types of data are input into the network, and the hierarchical analysis method is used to determine the weights of each type of data. Finally, the feasibility of the ideological and political education effectiveness assessment model proposed in this paper is validated through examples.

II. Assessment of the effectiveness of ideological and political education combining facial expressions and behavioral recognition

II. A. Student facial expression recognition model based on deep attention networks

II. A. 1) Model Framework

Given that students' facial expressions are often obscured in ideological and political education classroom settings, the loss of facial expression information from obscured areas inevitably affects the learning of facial expression features. Additionally, using a single convolutional neural network to learn student facial expression features cannot automatically focus on the effective regions of facial expressions, resulting in the inability to obtain effective facial expression information. Therefore, this paper proposes a student facial expression recognition model based on a deep attention network, with the model structure shown in Figure 1. This facial expression recognition model is

primarily divided into four parts: facial expression feature learning, attention feature weight allocation, facial expression feature fusion, and facial expression classification.

First, the point facial images in the classroom teaching video frames are cropped and occluded, and the cropped and occluded facial images are divided into five streams along with the original facial images. The facial expression features are extracted by the respective branch networks of the student facial expression feature learning module based on a deep attention convolutional neural network. Then, through the attention feature weight allocation module, different weights are assigned to the features learned by the sub-network based on the self-attention mechanism, resulting in new attention weights for each sub-network feature set. Constraint loss functions are added to the new attention weights to prevent the occluded path from becoming the sub-network with the highest weight. Finally, all branch expression features are integrated through the expression feature fusion module, which combines the features and weights from each branch into a global feature representation of the facial expression. The global feature representation is the sum of the weighted attention features from each branch, i.e., the final global representation of the facial expression. At the end of the network, a softmax classifier [33] is used to classify the student's facial expression, thereby completing the construction of the entire model.

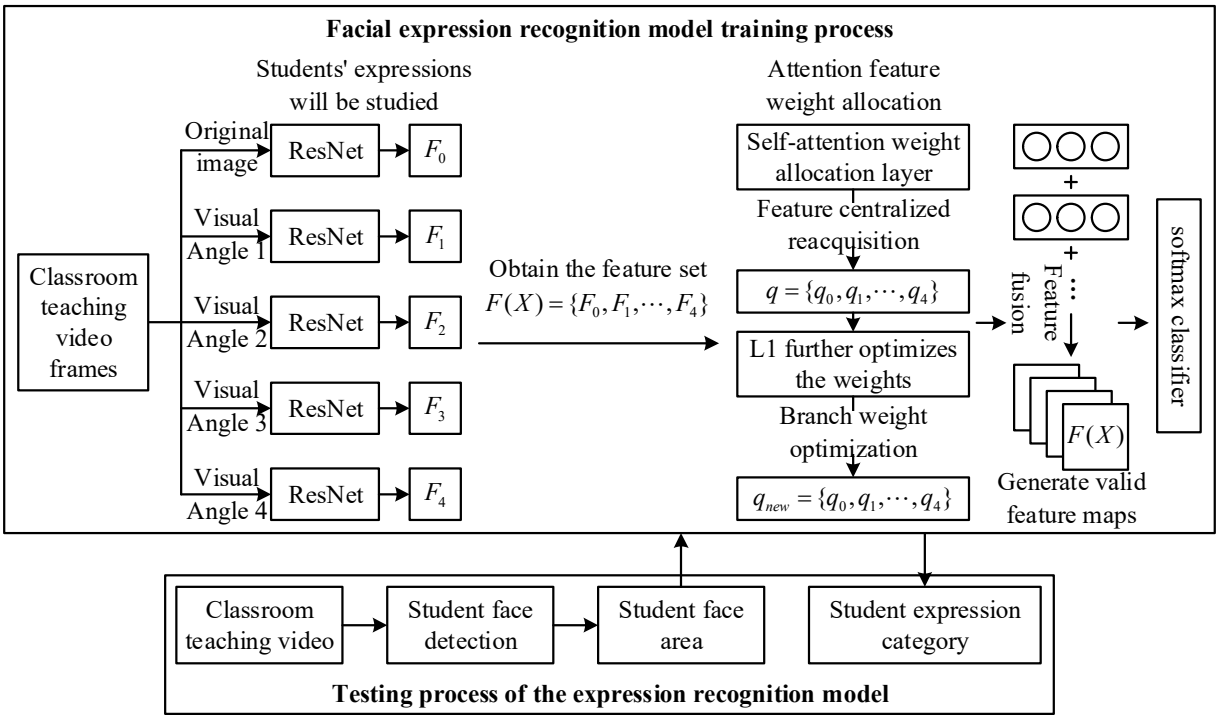

Figure 1: the student expression recognition model

II. A. 2) Learning student facial expression features based on deep attention networks

Due to the high probability of facial obstruction in ideological and political education classrooms, leading to the loss of facial expression information, this paper constructs a deep convolutional neural network based on the self-attention mechanism for learning student facial expression features. To further integrate local facial expression features, obstructed facial expression features, and overall facial expression features, this paper constructs five branches to extract local features, obstructed features, and overall features, respectively. Each branch network consists of five identical convolutional neural networks, with a fully connected layer and activation function at the end of the branch network to capture the weights of each branch network. Additionally, a constraint loss function is introduced during the optimization of the weights of each branch to further adjust the weights of each branch, achieving the fusion of local and overall features and obtaining effective facial expression feature maps.

First, input a face image into the network, copy it to obtain X_o, then crop and occlude X_o to obtain $X_i \sim X_i$ is obtained. Each image is then input into the same branch convolutional neural network to extract branch-specific facial expression features, where $X=[F_0,F_1,\cdots,F_4]$ represents the set of facial expression features obtained from each branch. The facial expression feature set is input into the feature weight allocation layer, where each image feature F_i is encoded as a global feature z_i. Two fully connected layers are used to learn the attention weights

for different student facial expression features. The formula for calculating the attention weights for student facial expression features is as follows:

$$q_i = S(W_2 * R(W_1 * z_i)) \tag{1}$$

where, q_i is the weight of each branch's facial expression feature, W_1 and W_2 are the weights of the fully connected layer, R is the ReLU activation function, and S is the Sigmoid activation function. The calculated attention weights are multiplied by the features learned through the convolutional neural networks of each branch to obtain the optimized global facial expression features. The formula for calculating the global facial expression features output by the self-attention mechanism layer is as follows:

$$F_m = \frac{1}{\sum_{i=0}^{c} q_i} \sum_{i=0}^{c} q_i * F_i \tag{2}$$

Among these: F_m represents the global facial expression features adjusted via the self-attention mechanism, F_i denotes the student facial expression features learned by each branch convolutional neural network, and c represents the number of branches.

The resulting F_m is a global facial expression feature that combines local and global information. Facial expression features are optimized by a deep attention network to assign different weights to different regions of the face, filtering out redundant information and overcoming the impact of face occlusion on facial expression recognition.

II. A. 3) Constrained Loss and Label Loss Functions

In order to further constrain the proportion of occluded images in each branch, this paper improves the max-margin function [34] so that the weight of the occluded branch is always less than the maximum weight in each branch. The improved constraint loss function formula is as follows:

$$L1 = \max(0, margin - q_{\max} + q_l) \tag{3}$$

Among these: $q_{\max}$ is the maximum weight of each branch, q_t is the weight of the occluded branch, and $margin$ is the threshold.

During training, the weight distribution mechanism of self-attention for each branch can initially learn the importance of each branch in the global features. However, artificial occlusion of facial images inevitably causes the image to lose a certain amount of information. Therefore, constraints on the occluded branch are particularly important. By further limiting the minimum weight of the occluded branch, the loss of expression information caused by artificial occlusion can be compensated for. At the same time, combining classification loss with constraint loss optimizes the learned expression features. The classification loss function is as follows:

$$L2 = (y \log y' - (1-y)\log(1-y')) \tag{4}$$

where, y represents the expected true emotion label, and y' represents the expected predicted emotion label. The final constraint loss function is combined with the classification loss function to optimize the emotion classification model. The total loss function is optimized as follows:

$$L = L1 + L2 \tag{5}$$

The improved constrained loss function enhances the effectiveness of the self-attention mechanism. Through this constrained function, the weights of each branch are further optimized, thereby further optimizing the global facial expression feature representation.

II. A. 4) Facial expression recognition of students in classroom teaching videos

This paper proposes a student facial expression recognition model for classroom videos based on a deep attention network. The network architecture combines a deep convolutional neural network with an attention mechanism to overcome the impact of occlusion on expression information loss in real-world scenarios, thereby enabling the extraction of facial expression features for each student. Compared to conventional deep convolutional neural networks, the performance of the entire student classroom expression recognition model has been improved.

During network construction, the model first learns student facial expression features through the deep attention network; then, by reasonably allocating weights to different regions of student facial expressions, it learns more rich and effective facial expression feature representations; finally, a softmax classifier is used at the end of the network to classify facial expressions, thereby completing the entire model construction.

When performing student classroom facial expression recognition, we first extract key frames from classroom video data with people present, and then perform operations such as grayscaling and image enhancement on the extracted key frames. Next, we perform student face detection and select the face with the largest region of interest. Finally, we extract facial expression features from the student's face for prediction, obtain the probabilities of various expressions, and select the expression category with the highest probability as the output.

II. B.Student behavior recognition algorithm based on multi-task learning

II. B. 1) Student Behavior Recognition Algorithm

The Multi-Task Classroom Behavior Recognition Network (MCBRN) is a classroom behavior detection method based on multi-task learning, which combines object detection and pose estimation tasks.

First, key frames from classroom teaching videos are used as initial input and fed into a body detector (YOLOv3-SPP) [35] to obtain individual student regions. Next, the Multi-Task Heatmap Network (MTHN) module generates a shared heatmap Y. Each task has a different mapping relationship with the heatmap Y. $Block_p$ maps Y to keypoints P_1 and offsets O_1, $Block_d$ maps Y to the target center point P_2, offset O_2, and width W_h; Finally, the behavior vector E_p and object vector E_o are processed through the Det and DNN modules to identify student behavior.

II. B. 2) MTHN Module

The MHTN module maps the input image X to a shared heat map Y:

$$Y = MHTN(X) \tag{6}$$

Among them, $X \in R^{H \times W \times 3}$ is the input of the module, where H, W represent the height and width of the input, respectively, $Y \in [0,1]^{\frac{H}{3} \times \frac{W}{3} \times C}$ is the output of the module, and C represents the number of heat map channels. S denotes the relative downsampling scale of the heatmap relative to the input.

This module is based on a feature pyramid network. By progressively downsampling to expand the receptive field, high-level semantic features are obtained. MHTN names the feature downsampling layers as $Conv_i$. The feature transformation is shown in Formula (7):

$$F_i = Conv_i(X) \tag{7}$$

Among them, $F_i \in R^{\frac{H}{27} \times \frac{W}{27} \times C_i}$ represents the feature output of the i th downsampling layer, and C_i is the number of feature channels in the i th layer.

After obtaining the transformed features from each sampling layer, the low-resolution high-level semantic features are upsampled to high-resolution features using a 1×1 convolution layer $(conv_{1\times1})$ and an upsampling transformation $(2 \times Up)$. During the upsampling process from high-level low-resolution feature maps to high-level high-resolution feature maps, lower-level features are continuously fused to enhance information exchange between multi-scale features at different scales. First, $conv_{1\times1}$ is used to compress the number of channels in F_j, $j \in [3,5]$ to the same channel depth as F_i, $i \in [2,4]$, then expands the feature resolution using the $2 \times Up$ method, and finally adds F_i and the transformed F_j to form a new feature map. That is:

$$F_{i,j} = F_i + 2 \times Up(conv_{1\times1}(F_j)) \tag{8}$$

$$F_{55} = F_5 \tag{9}$$

Before feature fusion, $F_{i,j}$ is sampled to the same scale as the heat map. The features $F_{3,4}, F_{4,5}, F_{55}$ are upsampled to 2, 4, and 8 times the size of $F_{2,3}$, respectively. To reduce feature loss during the upsampling process, the features after each doubling of the upsampling are combined with the features from the previous layer. Taking

F_{45} as an example, first perform 2x upsampling on F_{45}, then add it to $F_{3,4}$, and finally perform another 2x upsampling to obtain a feature map of the same scale as Y.

$$\begin{aligned} U_{23} &= F_{2,3} \\ U_{34} &= 2\times Up(F_{3,4}) \\ U_{45} &= 2\times Up(F_{3,4} + 2\times Up(F_{4,5})) \\ U_{55} &= 2\times Up(2\times Up(F_{4,5} + 2\times Up(F_5)) + 2\times Up(F_{4,5})) \\ Y &= concat(U_{23}, U_{34}, U_{45}, U_{55}) \end{aligned} \tag{10}$$

MHTN overlays the upsampled feature maps of $F_{i,j}$ and outputs a heatmap $Y \in [0,1]^{\frac{H}{S}\times\frac{W}{S}\times C}$, where C is the number of channels in the heatmap and S is the downsampling factor of the output.

II. B. 3) Multi-task heat map processing

Pose estimation: The purpose of human pose estimation algorithms is to detect the positions of N human keypoints in an image, including the nose, ears, shoulders, elbows, wrists, hips, and legs. Using a $Block_p$ composed of 3×3 convolution, ReLU, and 1×1 convolution, the heatmap Y is mapped to the keypoint heatmap P_1 and offset O_1:

$$(P_1, O_1) = Block_p(Y) \tag{11}$$

Among them, $P_1 \in [0,1]^{\frac{H}{S}\times\frac{W}{S}\times C_1}$ and $C_1 = 17$ represent the number of key points on the human body. $O_1 \in [0,1]^{\frac{H}{S}\times\frac{W}{S}\times C_2}$ $C_2 = 2$ respectively represent the offset values for the width and height of the keypoints. $S = 4$ denotes the downsampling scale of the heatmap relative to the input.

Assume that the input X is composed of pixel points (x, y), and the true labels of the pose keypoints are $(x_p, y_p), p \in [1, C_1]$. During the inference stage, the argmax function is used to convert P_1 into the predicted keypoint coordinates $(\hat{x}_p, \hat{y}_p)$ with $p \in [1, C_1]$ converts O_l to the predicted keypoint width and height offset distances (w_p, h_p):

$$(\hat{x}_p, \hat{y}_p) = \arg\max(P_1) \tag{12}$$

$$(w_p, h_p) = \arg\max(O_1) \tag{13}$$

Object detection: For object detection, anchor-free detection algorithms such as CenterNet can directly use heatmaps generated from feature maps without discretizing the data using default bounding boxes. The center point of an object is directly converted into a two-dimensional Gaussian distribution, and its maximum point is the center point of the object. The network maps the heatmap Y through $Block_d$ to different branches, where P_2 represents the center point heatmap, O_2 represents the bias, and W_h represents the width and height of the object bounding box:

$$(P_2, O_2, W_h) = Block_d(Y) \tag{14}$$

where $P_2 \in [0,1]^{\frac{H}{S}\times\frac{W}{S}\times C_3}, O_2 \in [0,1]^{\frac{H}{S}\times\frac{W}{S}\times 2}, W_h \in [0,1]^{\frac{H}{S}\times\frac{W}{S}\times C}$, where C_3 denotes the number of target detection categories.

Assume that the true label of the target center is (x_d, y_d) and the width and height of the target box are $Z_d = (x_{\max} - x_{\min}, y_{\max} - y_{\min})_d$, where $d \in [1, C_3]$, and $\{x_{\min}, y_{\min}), (x_{\max}, y_{\max})\}$ denotes the true object bounding box coordinates. In the inference stage, the argmax function is used to convert P_2 to the target center coordinates $(\hat{x}_d, \hat{y}_d)$ with $d \in [1, C_3]$ converts O_2 to the center point width and height offset distances (w_d, h_d) and converts W_h to the predicted box width and height $\hat{Z}_d = (E_w, E_h)$.

$$\begin{aligned} (\hat{x}_d, \hat{y}_d) &= \arg\max(P_2) \\ (w_d, h_d) &= \arg\max(O_2) \\ (E_w, E_h) &= \arg\max(W_h) \end{aligned} \tag{15}$$

Multi-task loss function: During training, the multi-task network simultaneously performs human pose estimation and object detection tasks. This paper references the CenterNet network design for the loss function. The loss function of the pose network consists of keypoint loss and bias loss, while the object detection network consists of object loss, bias loss, and width-height loss L_{size}. As shown in Equation (16), Gaussian kernels are used to generate heatmap labels P_p and P_d for keypoints and object center points, respectively.

$$\begin{aligned} P_p &= \exp(-\frac{(x-x_p)^2+(y-y_p)^2}{2\sigma^2}) \\ P_d &= \exp(-\frac{(x-x_d)^2+(y-y_d)^2}{2\sigma^2}) \end{aligned} \tag{16}$$

The keypoint loss function is shown in Equation (17), where N_p denotes the number of human keypoints.

$$L_{pp} = \frac{1}{N_p}\sum_{n=0}^{N_p}\sum(P_1 - P_p)^2 \tag{17}$$

To compensate for the bias caused by data dispersion when calculating the predicted key points, the network introduces a bias loss during key point estimation to compensate for this error. Ideally, we want $L_{op}=0$. During training, given $\frac{(x_p,y_p)}{S}-\left\lfloor\frac{(x_p,y_p)}{S}\right\rfloor$, the model strives to make the predicted bias equal to this value. During the testing phase, the predicted keypoint coordinates $(\hat{x}_p,\hat{y}_p)$ and the keypoint width and height offsets (w_p,h_p) can be obtained, allowing the true keypoint coordinates to be calculated after error correction.

$$L_{op} = \frac{1}{N_p}\sum\left|(w_p,h_p)-(\frac{(x_p,y_p)}{s}-\left\lfloor\frac{(x_p,y_p)}{s}\right\rfloor)\right| \tag{18}$$

The loss function for object detection consists of three parts: heatmap loss L_{pd}, offset loss L_{od}, and width-height loss L_{size}. Similar to keypoint detection, during the inference stage, the center point coordinates of the object $(\hat{x}_d,\hat{y}_d)$ are obtained, where $d\in[1,C_3]$ center point width and height offsets (w_d,h_d), and target box prediction width and height (E_w,E_h). Here, N_d represents the object detection category.

$$\begin{aligned} L_{pd} &= \frac{1}{N_d}\sum_{n=0}^{N_d}\sum_{m}(P_2-P_d)^2 \\ L_{op} &= \frac{1}{N_d}\sum\left|(w_d,h_d)-(\frac{(x_d,y_d)}{s}-\left\lfloor\frac{(x_d,y_d)}{s}\right\rfloor)\right| \\ L_{size} &= \frac{1}{N_d}\sum|\hat{Z}_d - Z_d| \end{aligned} \tag{19}$$

The total loss L of the multi-task network is the sum of the pose estimation loss and the object detection loss. where α and $1-\alpha$ represent the weights of the two losses, respectively. In the experiment, $\alpha=0.2$ is set.

$$L = \alpha(L_{pp}+L_{op})+(1-\alpha)(L_{od}+L_{size}+L_{pd}) \tag{20}$$

II. B. 4) Student Behavior Recognition

The MCBRN network incorporates six high-engagement actions of students in the classroom into the behavior recognition network, including raising hands, listening to lectures, reading books, standing up, leaning on desks, and playing with mobile phones. In classroom scenarios, some actions are difficult to distinguish from others based solely on posture. For example, listening and reading are hard to differentiate using only keypoint information, but if visual information corresponding to books and pens is available, they can be easily separated. This paper employs a behavior recognition method combining pose vectors and metric vectors.

In pose-based recognition, since desks often obstruct students' knees and feet, this paper restricts the keypoints used to represent behavior to the trunk, head, and arm regions, totaling 15 valid keypoints, with invalid keypoints set to zero. Ultimately, each student is represented by a 30-dimensional behavioral feature vector E_p.

$$E_p = \{X_1, Y_1, X_2, Y_2, ..., X_{15}, Y_{15}\}$$
$$(X_n, Y_n) = (\hat{x}_n + w_n, \hat{y}_n + h_n), n \in [1,15] \tag{21}$$

The detected target M objects detected on the input image X, represented by the vector $\{E_o\}_m$, where $\{E_x, E_y\}$ are the center points of the objects, and $\{E_w, E_h\}$ are the width and height of the objects.

$$\{E_o\}_M = \{E_x, E_y, E_w, E_h\}_m, m \in [1, M]$$
$$\{E_x, E_y\}_m = \{\hat{x}_d + w_d, \hat{y}_d + h_d\}_m \tag{22}$$

This paper models the distance relationship between key points and objects, calculating the distance vector $\{E_d\}_m$ for each target center point to the key point, where $n \in [1,15], m \in [1, M]$.

$$\{E_d\}_m = \{d_o^n\}_m$$
$$d_o^n = \sqrt{(X_n - E_x)^2 + (Y_n - E_y)^2} \tag{23}$$

The behavioral feature vector and the metric feature vector are combined to obtain the fusion feature vector $E_{pd} = \{E_p, E_d\}_m$. The classification module FCS maps the vectors E_p and E_{pd} to behavior scores, which are then converted into probability distributions using the Softmax function. FCS is a classifier composed of three fully connected layers with 128 dimensions and 7 dimensions. The network defines the predicted probability distributions of the behavior vector and the combined feature vector as S_p and S_{pd}, respectively, and defines the product of the two as the behavior recognition network score $S_{finally}$.

$$S_{finally} = S_p \times S_{pd} \tag{24}$$

II. C.Determination of evaluation indicator weights

This paper collects adult education classroom videos as experimental data, with each video lasting approximately 10 minutes, in MP4 format, with a resolution of 856×480, a frame rate of 30 frames per second, and 500 classroom images obtained. Additionally, the attention evaluation sets V_1, V_2, V_3 are each assigned score thresholds S_1, S_2, S_3 of 100, 75, and 60, respectively. First, the weights of the first-level and second-level factors are determined using the analytic hierarchy process. Then, the algorithm proposed in this paper is used to identify students' expressions and behaviors in college ideological and political education classroom videos. Finally, the students' attention levels are calculated and analyzed based on the identification results and the determined weights.

This paper employs the Analytic Hierarchy Process (AHP) to determine the weights of each factor. This method is a research approach that bridges the gap between subjective and objective evaluation, primarily used for decision-making involving multiple factors. It clarifies fuzzy concepts to determine the weight coefficients of all factors, following these basic steps:

1) Construct a pairwise comparison judgment matrix:

The judgment matrix is constructed to quantify the relative importance of indicators at each level in the hierarchical structure, typically using a 1-9 scale. The relative importance between each pair of indicators is compared to obtain the judgment matrix.

2) Calculate the initial weight coefficients $\overline{w}_i$:

$$M_i = \prod_{j=1}^{n} u_{ij}, i, j = 1, 2, \cdots, n \tag{25}$$

$$\overline{w}_i = \sqrt[n]{M_i}, i = 1, 2, \cdots, n \tag{26}$$

Normalize the judgment matrix and calculate the eigenvectors and maximum eigenvalues using the square root method:

$$w_i = \frac{\overline{w}_i}{\sum_{j=1}^{n} \overline{w}_j}, j = 1, 2, \cdots, n \tag{27}$$

$$\lambda_i = \sum_{j=1}^{n} (u_{ij} w_j / w_i) \tag{28}$$

$$\lambda_{\max} = \sum_{i=1}^{n} \lambda_i / n \tag{29}$$

3) Perform consistency testing on the matrix, calculate the consistency index CI and the test coefficient CR:

$$\begin{cases} CI = (\lambda_{\max} - n) / (n-1) \\ CR = CI / RI \end{cases} \tag{30}$$

In this context, n denotes the order of the judgment matrix, and RI represents the average random consistency index. If $CR \le 0.1$, the judgment matrix is deemed to have satisfactory consistency; otherwise, adjustments are made until $CR \le 0.1$ is satisfied.

III. Examples of evaluating the effectiveness of ideological and political education in universities

III. A. Student Behavior Recognition Experiment and Results

III. A. 1) Experimental Data Set

Experimental environment: CPU Intel Xeon(R) E5-2640, 8G memory, GPU NVIDIA RTX2070Super, Pytorch deep learning framework, and OpenPose open source library. The experimental data sets for model training and verification include object detection data sets and behavior recognition data sets, specifically:

(1) Object detection dataset: To train and test the student location detection model, the occlusion detection dataset CityPersons is used. The training set and test set contain 3,000 and 600 images, respectively, each with a resolution of 2048×1024, featuring diverse occlusion forms, and providing full-body bounding boxes and visible-part bounding boxes for human targets.

(2) Student Classroom State Dataset: Before practical application, the student state recognition model needs to be trained and tested. Since there are currently no standard public datasets available domestically or internationally, this paper selected 500 volunteers from X University as the data source. Each student was filmed performing six classroom state actions: raising hands, listening to lectures, reading books, standing, leaning on desks, and playing with mobile phones. The dataset NEPU was constructed through data annotation. The dataset includes a total of 5,000 images with a resolution of 1920×1080, divided into a training set and a test set at a ratio of 7:3.

III. A. 2) Experimental Analysis Results

To ensure the validity of the experimental comparison, five independent random experiments were conducted under the same experimental conditions, and the experimental results represent the average recognition accuracy rate of multiple experiments. Based on the experimental environment, the epoch was set to 150, and the mini-batch was set to 20. Precision and recall are commonly used evaluation metrics in machine learning classification problems. Precision refers to the ratio of correctly predicted samples among all samples predicted as 1, while recall refers to the ratio of correctly predicted samples among all true samples. The comparison results for precision and recall of SVM and the model in this paper are shown in Table 1.

Table 1: Student behavior recognition statistics indicator

	SVM		This model	
	Recall rate R	Precision P	Recall rate R	Precision P
Hand up	0.863	0.819	0.941	0.889
lecture	0.789	0.817	0.881	0.914
Read a book	0.778	0.817	0.858	0.902
standing	0.888	0.839	0.955	0.905
Party table	0.888	0.816	0.924	0.897
Play phone	0.743	0.839	0.854	0.923

Figures 2 and 3 show the confusion matrices for the recognition of six classroom states using SVM and the model proposed in this paper, respectively. It can be clearly seen that for the three behaviors with relatively distinct skeleton joint features—“raising hand,” “standing,” and “leaning on the desk”—the recognition accuracy is high, with the

highest accuracy achieved for “leaning on the desk,” reaching 91% for SVM and 95% for the model proposed in this paper. For the three behaviors—“listening to the lesson,” “reading a book,” and “playing with a phone”—where the joint feature distinctions are relatively low, the accuracy is slightly lower. Additionally, the model proposed in this paper demonstrates a significant improvement in recognition accuracy for all six states compared to the classic machine learning SVM model.

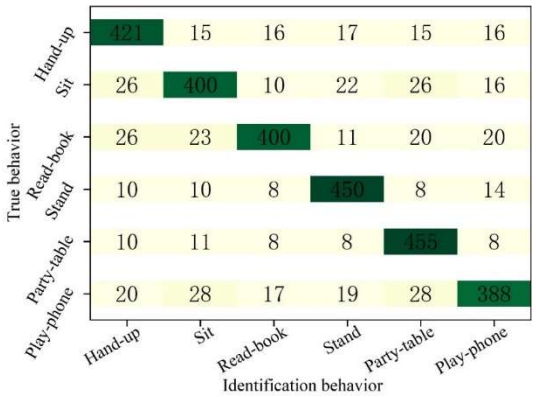

Figure 2: SVM is the confusion matrix of six class status recognition

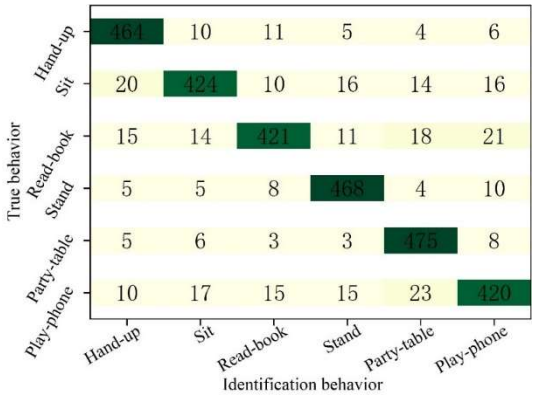

Figure 3: This paper models the confusion matrix of six class status recognition

III. B. Student facial expression recognition experiment and analysis of results

III. B. 1) Introduction to the dataset

The Fer2013 dataset contains 35,886 facial expression images, each consisting of a grayscale image with a fixed size of 48x48. The dataset has seven expression categories: surprise, happiness, disgust, anger, fear, sadness, and neutral. This dataset will be used in this paper.

III. B. 2) Analysis of experimental results

To validate the effectiveness of the model proposed in this paper, experiments were conducted on the same dataset and compared with the mini_Xception network, DNNRL, and Tc Net. The experimental results are shown in Table 2. The results show that the model proposed in this paper achieved the highest experimental accuracy of 74.56%, which is the highest among the four models.

Table 2: Comparison of experimental results accuracy

Model	Accuracy rate/%
This model	74.56
mini _Xception	63.51
DNNRL	71.23
TcNet	68.46

This paper compares the proposed network with other networks on the same dataset, performing training and testing separately. After the same number of training iterations, the convergence of the loss for emotion recognition is shown in Figure 4. It is evident that the model proposed in this paper converges the fastest, reaching convergence after 15 epochs.

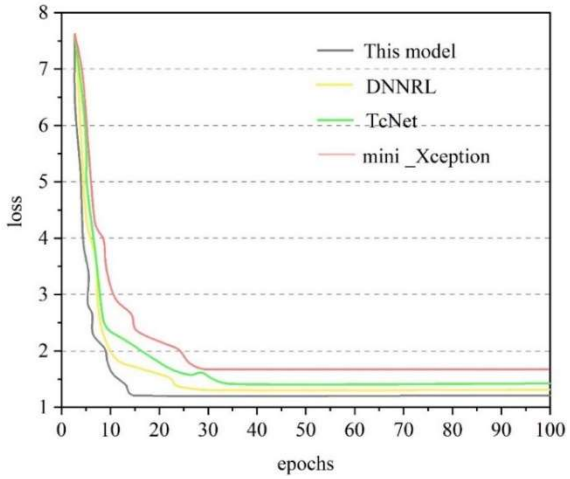

Figure 4: The loss convergence of expression recognition

Figure 5 shows the confusion matrix for the recognition of seven emotions using the model described in this paper. It can be clearly seen that the recognition accuracy for the three emotions of “surprise,” “neutral,” and “sadness” is relatively high, with ‘sadness’ having the highest recognition accuracy at 75.8%, while the recognition accuracy for “fear” is slightly lower at 63%.

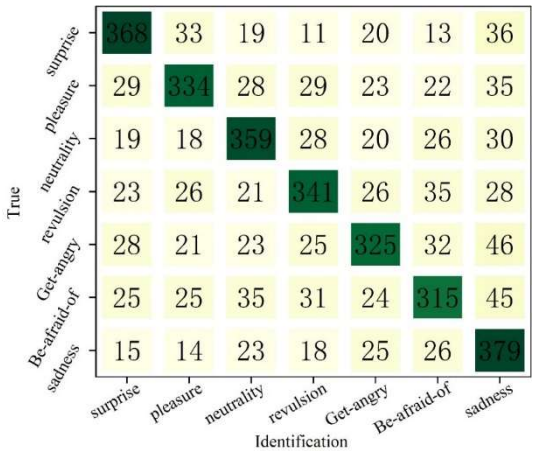

Figure 5: This paper models the confusion matrix of seven expression recognition

III. C. Assessment of the effectiveness of ideological and political education integrating students' expressions and behaviors

III. C. 1) Comparison of assessment accuracy under different weightings

A method for evaluating the effectiveness of ideological and political education that integrates students' facial expressions and behavior involves combining students' facial expressions and behavior to derive a comprehensive evaluation value. Therefore, it is necessary to calculate the probability values of positive behavior and positive facial expressions, then assign corresponding weights, and finally calculate the comprehensive evaluation value. The higher the comprehensive evaluation value, the more obvious the positive feedback in the classroom, and the better the overall classroom state; the lower the comprehensive evaluation value, the more obvious the negative feedback in the classroom, and the worse the overall classroom state. Since this method requires assigning a set of reasonable weight values to students' facial expressions and behaviors for integration, it is necessary to test the evaluation performance under multiple different weight combinations. Considering that students' facial expressions more intuitively and accurately reflect their emotions compared to their behavioral states, facial expressions should

have a stronger dominant role in comprehensive evaluations, resulting in more accurate final evaluation outcomes. Therefore, when integrating both for comprehensive assessment, to highlight the dominant role of facial expression recognition results in the final assessment outcome, the weighting value for facial expressions should be greater than that for behavioral states. During testing, student facial expressions were categorized into seven types, and student behaviors into six types. A total of 40 classroom videos were selected as test data, and assessment tests were conducted under four different weighting value combinations. Weighting combination 1 assigned a weight of 0.8 to facial expression recognition and 0.2 to behavioral recognition. Combination 2 assigned equal weights of 0.5 to both. Combination 3 assigned a weight of 0.6 to facial expression recognition and 0.4 to behavioral recognition. Combination 4 assigned weights of 0.55 and 0.45 to facial expression recognition and behavioral recognition, respectively. The results of the first 20 test groups are shown in Table 3.

It can be seen that when a weight of 0.6 is assigned to facial expression recognition results and a weight of 0.4 is assigned to behavioral recognition results, the recognition accuracy of the method for assessing the effectiveness of ideological and political education by integrating students' facial expressions and behaviors is relatively high, reaching 85%, which is significantly higher than the facial expression recognition accuracy of the other three weight combinations. Therefore, this is determined as the final weight allocation strategy.

Table 3: The evaluation of the thought of political education under different weights

Video number	The number of people identified	The evaluation grade of the education effect	Classroom evaluation results under different weights			
			Exp.weight: 0.8 Beh.weight: 0.2	Exp.weight: 0.5 Beh.weight: 0.5	Exp.weight: 0.6 Beh.weight: 0.4	Exp.weight: 0.55 Beh.weight: 0.45
1	8	A	A	B	A	A
2	4	B	A	B	B	B
3	6	C	C	C	B	B
4	9	A	B	A	A	A
5	7	B	C	A	B	A
6	8	B	A	B	A	B
7	9	B	B	A	B	C
8	7	B	B	B	B	B
9	10	B+	C-	B	B+	B
10	12	A+	A+	A+	A+	A
11	11	A+	A+	A+	A+	A+
12	9	C	C	C	C	C
13	10	C	B	C	C	B
14	13	A	B	B	A	A
15	15	A	B	B	A	A
16	11	B+	A+	B+	B+	C+
17	8	C	B	C	C	C
18	9	A+	A+	A+	A+	A+
19	10	B	B	A	C	B
20	11	B	B	C	B	C
Acc/%	/	/	50%	60%	85%	60%

III. C. 2) Comparative evaluation experiments under different evaluation methods

Based on the weighting strategy for allocating values in the intelligent assessment algorithm that integrates student facial expressions and behavior, as determined by the above experiments, 100 classroom videos were selected as test data. These 100 test videos were divided into 10 groups, with 10 test videos in each group. Experiments were conducted to compare the three assessment methods: student facial expressions, student behavior, and the integration of student facial expressions and behavior, on the 10 groups of classroom video data. When conducting assessments based on students' classroom facial expressions and classroom behaviors, the number of students exhibiting positive expressions and positive behaviors was obtained, and the ratio of this value to the total number of identified students was calculated. Finally, this ratio was compared with the threshold for grade determination in the intelligent assessment algorithm that integrates students' facial expressions and behaviors to complete the assessment state mapping, ensuring consistency in the grading criteria. The experimental results are shown in Table 4. It can be seen that the accuracy rate of classroom assessment based solely on expressions was 60.09%, the average accuracy rate of classroom assessment based on behavior was 57.63%, and the average accuracy

rate of the intelligent assessment method combining students' expressions and behavior reached 85.44%, significantly higher than the other two methods.

Table 4: Comparison of evaluation accuracy under different evaluation methods

Video number	Based on expression evaluation accuracy/%	Behavior based evaluation accuracy/%	The evaluation accuracy of the student's expression and behavior/%
1	58.9	58.4	85.6
2	59.4	56.6	89.7
3	61.5	59.9	86.4
4	62.6	65.4	86.9
5	68.4	56.8	87.8
6	54.3	52.6	88.9
7	55.6	53.4	79.8
8	54.9	51.8	82.3
9	61.5	66.1	85.4
10	63.8	55.3	81.6
Average accuracy/%	60.09	57.63	85.44

IV. Analysis of the effectiveness of the application of the ideological and political education effectiveness assessment model

IV. A. Experimental Design

To further validate the accuracy and practicality of attention evaluation teaching methods in actual classroom teaching processes, and to explore the potential shortcomings of traditional attention evaluation teaching methods, this study employs an accurate experimental method to conduct classroom teaching experiments. This paper selects a university social studies course as the research object, as university education serves as a crucial foundational stage in students' academic careers, and the university stage is a period when attention spans are most unstable. Therefore, studying students' attention levels during this stage holds significant practical value.

The primary research subject of this study is a university-level social science course. By incorporating attention evaluation methods into teaching, teachers can obtain more emotional information about students, thereby gaining insight into their attention levels and learning states. Through analyzing students' learning states, teachers can understand their current learning conditions and promote their healthy development.

Before the experiment, the testing equipment must be checked to ensure the model is functioning normally. During the experiment, teachers should not interfere with students' normal learning habits to ensure their learning states remain stable. After completing the experiment, the reliability of the attention evaluation model should be analyzed to study its effectiveness.

IV. B. Analysis of experimental results

This research method comprehensively evaluates the quality of students' learning in ideological and political education classrooms by combining behavioral posture and facial expression recognition to analyze the overall teaching quality, calculating the students' attention level, participation level, and confusion level during ideological and political education classroom learning. To enable teachers to intuitively understand the teaching situation in ideological and political education classrooms, the model visually represents the results in graphical form. If the model indicates that students' attention levels, participation levels, and confusion levels are relatively low during the learning process in ideological and political education classrooms, this suggests that current learning efficiency is suboptimal, necessitating adjustments to teaching strategies, improvements to teaching content, and enhancements to teaching quality.

To validate the accuracy of the model for assessing the effectiveness of ideological and political education for students, structured observation methods were used to statistically analyze students' attention levels during each time segment by reviewing classroom learning videos. The analysis determined students' attention levels, participation levels, and confusion levels at each time point. The actual statistical results were compared with the model's detection results to verify the accuracy of the model's evaluations. This study selected students' learning situations within a 20-minute period for comparison, recording their learning situations every minute, and finally compared and analyzed the differences between the attention evaluation detection model and the actual teaching effectiveness. Through experimental analysis, it was found that students' attention was primarily focused on the initial stage of the course, and as time progressed, their learning state exhibited a trend of first increasing and then

gradually decreasing. Therefore, teachers need to continuously adjust strategies to enhance student interest and improve teaching quality. Figures 6, 7, and 8 show the comparison results of student attention levels, student participation levels, and student confusion levels, respectively.

After class, in-depth discussions were conducted with instructors and students through interviews to comprehensively analyze the accuracy of the student ideological and political education effectiveness assessment model. Through interviews with instructors, it was found that instructors compared the results of the student ideological and political education effectiveness assessment with students' ideological and political stage exam scores. The analysis revealed that the student ideological and political education effectiveness assessment model has good predictive value for students' academic performance, with high accuracy in identification results and significant practical application value. Through interviews with students, it was found that students who watched video replays after class believed that the evaluation results of the model align with their learning state at the time and have high accuracy. Finally, both teachers and students agreed that the model is simple to operate, convenient to use, and has high accuracy, playing a positive role in promoting classroom teaching.

The experimental results showed that the method used in this study was consistent with manual statistical results. After comprehensive calculation, the accuracy rate of the student ideological and political education effectiveness assessment model was 94%. This demonstrates that the student ideological and political education effectiveness assessment method can effectively monitor students' classroom learning behavior, serving as an excellent formative assessment method. It enables teachers to fully grasp classroom teaching content and student learning status, thereby enhancing teaching quality while achieving significant application value for classroom instruction.

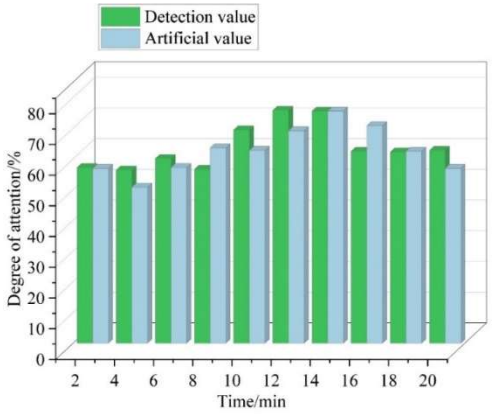

Figure 6: The degree of attention of the students was compared

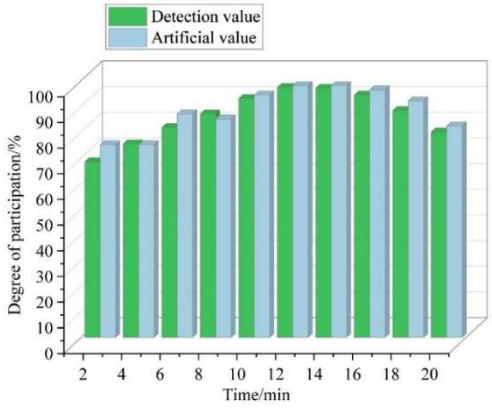

Figure 7: The results of the participation of the students

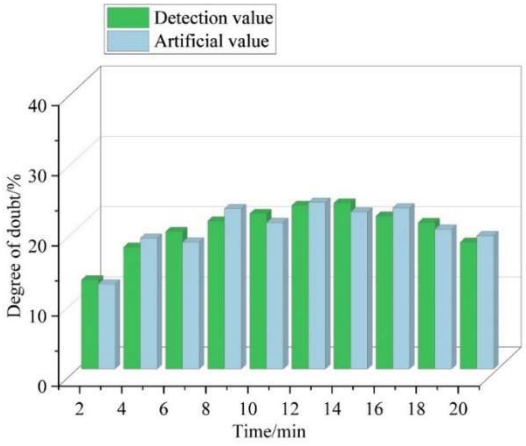

Figure 8: The students were puzzled by the degree of doubt

V. Conclusion

This paper employs biosensing technology to identify data from both the facial expressions and behaviors of college students, thereby evaluating the effectiveness of ideological and political education for college students.

The average accuracy rate of the intelligent teaching effectiveness evaluation method proposed in this paper, which integrates the facial expressions and behaviors of college students in ideological and political education classrooms, reached 85.44%, which is higher than that of evaluation methods that only input a single type of student data. Compared to methods that assess the effectiveness of ideological and political education classes based solely on facial expressions or behavior, the accuracy rate of this method has improved by more than 20%. This method can more comprehensively and objectively assess the effectiveness of students' ideological and political learning based on their facial expressions and behavioral states, avoiding the shortcomings of incomplete assessment results caused by inputting data from a single feature dimension. It is more meaningful for teachers to assess the effectiveness of ideological and political education classes.

The university ideological and political education effectiveness assessment model constructed in this paper, which integrates behavior recognition and facial expression recognition, was used to detect students' attention levels, participation levels, and confusion levels in ideological and political education classrooms. Through specific applications, it was found that the ideological and political education effectiveness assessment model designed in this paper can effectively monitor students' learning outcomes in ideological and political education classrooms. Over time, students' learning states exhibit a trend of first increasing and then decreasing, which aligns with actual student learning states. The accuracy of the evaluation of educational outcomes using the method proposed in this paper reached 94%, which is nearly identical to the accuracy rate of manual detection. This indicates that the student ideological and political education effectiveness evaluation method proposed in this paper can promptly provide teachers with comprehensive information about classroom teaching, enabling teachers to adjust their teaching strategies in a timely manner and thereby helping students achieve better learning outcomes.

References

[1] Pevzner, M. N., Petryakov, P. A., & Shaydorova, N. A. (2019). Civic education of university students in the context of information diversity. European Proceedings of Social and Behavioural Sciences.

[2] Nazira, D., & Kylych, K. (2024). Enhancing Civic Education and University Quality Management: An Innovative Approach. Journal of Ecohumanism, 3(8), 12032-12041.

[3] Claassen, R. L., & Monson, J. Q. (2015). Does civic education matter?: The power of long-term observation and the experimental method. Journal of Political Science Education, 11(4), 404-421.

[4] Fitzgerald, J. C., Cohen, A. K., Maker Castro, E., & Pope, A. (2021). A systematic review of the last decade of civic education research in the United States. Peabody Journal of Education, 96(3), 235-246

[5] Gumilar, A. T., Rahmat, R., Darmawan, C., & Anggraeni, L. (2025). The Effectiveness of Mandatory Curriculum Courses in Promoting Students' Civic Engagement in Higher Education. Edueksos Jurnal Pendidikan Sosial & Ekonomi, 14(01).

[6] Naval, C., Villacís, J. L., & Ibarrola-García, S. (2022). The transversality of civic learning as the basis for development in the university. Education Sciences, 12(4), 240.

[7] Burth, H. P. (2016). The contribution of service-learning programs to the promotion of civic engagement and political participation: A critical evaluation. Citizenship, Social and Economics Education, 15(1), 58-66.

[8] Gao, Y., Wang, B., Xu, P., Lv, Z., Jiao, J., & Liu, N. (2024). Big Data Analysis Based on the Evaluation of College Students' Civic Web. Journal of Combinatorial Mathematics and Combinatorial Computing, 120, 265-274.

[9] Sucipto, S., Setiawan, W., & Hatip, A. (2024). The effectiveness of collaborative learning on civic education problem-solving abilities based on cognitive styles. Research and Development in Education (RaDEn), 4(1), 149-161.

[10] EZE, A. A. (2016). Evaluation Processes/Challenges and Prospects of Implementing Civic Education Curriculum in Nigerian Schools. Journal of Resourcefulness and Distinction, 13(1), 49.
[11] Vigneshvar, S., Sudhakumari, C. C., Senthilkumaran, B., & Prakash, H. (2016). Recent advances in biosensor technology for potential applications–an overview. Frontiers in bioengineering and biotechnology, 4, 11.
[12] Ali, Q., Zheng, H., Rao, M. J., Ali, M., Hussain, A., Saleem, M. H., ... & Zhou, L. (2022). Advances, limitations, and prospects of biosensing technology for detecting phytopathogenic bacteria. Chemosphere, 296, 133773.
[13] Wang, L., & Tang, Z. (2025). Dynamic identification model of psychological state in Ideological and Political Education based on biosensing. Molecular & Cellular Biomechanics, 22(3), 1036-1036
[14] Fiore-Gartland, B., & Neff, G. (2016). Disruption and the political economy of biosensor data. Quantified: Biosensing technologies in everyday life, 101-22.
[15] Misera, J., Melchert, J., & Bork-Hüffer, T. (2024). Biosensing and Biosensors—Terminologies, Technologies, Theories and Ethics. Geography Compass, 18(11), e70007.
[16] Fang, Y., Chen, H., Tao, H., Tian, Y., Lu, L., & Cui, B. (2024). Practice and Exploration of Ideological and Political Education Reform in Course of Modern Food Testing Technology. International Journal Of Humanities Education and Social Sciences, 4(1).
[17] Zai, X. (2024). Leveraging Bio-Sensing Technology and IoT for Optimizing Spanish Vocabulary Instruction Across Chinese and Western Cultures: A Biotechnological Approach. Journal of Commercial Biotechnology, 29(3), 305-314.
[18] Zhang, W., Zhang, S., Wang, C., & Zhang, D. (2025). Improving ideological and political education with regular exercise programs: The contribution of the biosensor to cognitive development and student engagement. Molecular & Cellular Biomechanics, 22(1), 754-754.
[19] Wang, G. (2025). Research on the biological mechanism and biosensing monitoring of sports promoting ideological and political education. Molecular & Cellular Biomechanics, 22(3), 1313-1313.
[20] Zheng, W., & Wu, L. (2024). Construction of Ideological and Political Education of Professional Curriculum under the Background of Chinese Modernization. In SHS Web of Conferences (Vol. 190, p. 01027). EDP Sciences.
[21] Jin, Z., Wang, Q., Meng, F., & Xu, J. (2024). Research on monitoring college students' sports psychological stress response and ideological and political education intervention based on biosensors. Molecular & Cellular Biomechanics, 21(4), 537-537.
[22] Li, Y. (2024). Application research of psychological feedback monitored by biosensors in ideological and political education intervention for college students. Molecular & Cellular Biomechanics, 21(4), 589-589.
[23] Liu, Q., & Xu, W. (2023, March). The Construction of the Evaluation Index System of Curriculum Civic and Political Co-education in Private Universities. In 2nd International Conference on Education, Language and Art (ICELA 2022) (pp. 45-52). Atlantis Press.
[24] Omundi, E., & Okendo, E. O. (2018). Evaluation of the Effectiveness of Civic Education on Acquisition of Social Cohesion Competency among Secondary School Students in Uasin Gishu County, Kenya. International Journal of Scientific Research and Management, 6(04), 249-265.
[25] Han, Y., & Zeng, Y. (2023, June). Evaluation of Civic Education Effectiveness of WeChat Public Website of Universities Based on AHP Fuzzy Comprehensive Evaluation Method. In ITEI 2022: Proceedings of the 2nd International Conference on Internet Technology and Educational Informatization, ITEI 2022, December 23-25, 2022, Harbin, China (p. 406). European Alliance for Innovation.
[26] Zhu, Y. (2024). Assessment of civic education in universities from a multidimensional perspective: the Integration of OBE and CIPP models. International Journal of Information and Communication Technology, 25(11), 21-34.
[27] Huang, A. (2024). Speech Recognition Based on Mobile Biosensor Networks and Quality Evaluation of University Political Education. International Journal of High Speed Electronics and Systems, 2540128.
[28] Chen, S., Gong, C., & Pan, W. (2025). Construction of evaluation model of university ideological and political education effect based on biosensor technology. Molecular & Cellular Biomechanics, 22(1), 871-871.
[29] Zhao, R. (2025). Research on the effect of biosensing technology on the dissemination of health information in ideological and political education. Molecular & Cellular Biomechanics, 22(2), 1093-1093.
[30] Zheng, D., Wang, F., Wang, Y., & Hu, X. (2025). Emotion monitoring and feedback system for ideological and political education using biosensor technology. Molecular & Cellular Biomechanics, 22(3), 844-844.
[31] Lei, D., & Pi, Y. (2025). Biosensing technology based on biomechanics in psycho analysis: Improving the efficiency of ideological and political education. Molecular & Cellular Biomechanics, 22(2).
[32] Wang, Q. (2025). The Role of Emotional Biosensing Feedback in Evaluating the Effectiveness of Ideological and Political Education Teaching. International Journal of High Speed Electronics and Systems, 2540563.
[33] Ankai Wei,Sheng Guan,Na Wang & Shangrong Lv. (2024). Damage detection of jacket platforms through improved stacked autoencoder and softmax classifier. Ocean Engineering,306,118036-.
[34] Aram Khalid Y.,Lam Sarah S. & Khasawneh Mohammad T.. (2023). Cost-sensitive max-margin feature selection for SVM using alternated sorting method genetic algorithm. Knowledge-Based Systems,267,
[35] Su Xiaodong,Hu Jianxing,Chen Linzhouting & Gao Hongjian. (2023). Research on real-time dense small target detection algorithm of UAV based on YOLOv3-SPP. Journal of the Brazilian Society of Mechanical Sciences and Engineering,45(9).